PERGAMON

European Journal of Cancer 38 (2002) 1261–1270

European Journal of Cancer

www.ejconline.com

Regulation Of B16F1 melanoma cell metastasis by inducible functions of the hepatic microvasculature

H.H. Wang[a,d], A.R. McIntosh[b], B.B. Hasinoff[b,a], B. MacNeil[a], E. Rector[c], D.M. Nance[a], F.W. Orr[a,*]

[a]*Department of Pathology, Faculty of Medicine, University of Manitoba, Winnipeg, Manitoba, Canada R3E OW3*
[b]*Faculty of Pharmacy, University of Manitoba, Winnipeg, Manitoba, Canada R3T 2N2*
[c]*Department of Immunology, Faculty of Medicine, University of Manitoba, Winnipeg, Manitoba, Canada R3E OW3*
[d]*Division of Clinical Biochemistry & Immunology, Mayo Clinic, Rochester, MN 55905, USA*

Received 14 August 2001; received in revised form 5 December 2001; accepted 29 January 2002

Abstract

We have previously shown that circulating intravascular cells generally arrest by mechanical restriction in the hepatic sinusoids, causing rapid release of nitric oxide (NO) which is cytotoxic to these cells and inhibits their growth into metastatic tumours. Here, we present evidence that these NO-dependent cytotoxic mechanisms are susceptible to upregulation by lipopolysaccharide (LPS). Five$\times 10^5$ fluorescently labelled melanoma cells were injected into the mesenteric vein of C57BL/6 mice to effect their localisation in the hepatic microvasculature. Test mice were then given 1 mg/kg LPS intraperitoneally (i.p.) to activate the microvascular cells. By electron paramagnetic resonance (EPR) spectroscopy, the expression of NO in the liver was significantly increased by 8 h in the LPS-treated mice. The non-selective NO synthase inhibitor L-NAME inhibited the induction of NO by LPS, while its inactive enantiomer D-NAME had no significant effect. Using immunohistochemistry (IHC), iNOS-positive microvascular cells were detected in the terminal portal venule (TPV) region of the liver 8 h after LPS stimulation. LPS treatment also increased the retention of melanoma cells in the liver between 8 and 24 h, especially in the TPV region. Eight hours after cell injection, local expression of VCAM-1 and ICAM-1 was detected by double-label immunohistochemistry at the sites of tumour cell arrest. Expression of these adhesion molecules was enhanced in mice treated with LPS. Using flow cytometry, 98% of the B16F1 melanoma cells expressed VLA-4, the counter receptor of VCAM-1, and approximately 1.5% expressed LFA-1, the counter receptor of ICAM-1. LPS did not significantly alter the expression of either counter receptor on melanoma cells *in vitro* or *in vivo*. By DNA end-labelling, the rates of melanoma cell apoptosis were significantly increased from 8 to 24 h in the TPV region (but not in the sinusoids) of LPS-treated mice. Fourteen days after tumour cell injection, the LPS-treated mice had a significantly smaller hepatic metastatic tumour burden than the control mice. These data suggest that LPS can inhibit the metastasis of melanoma cells in the liver by inducing the expression of NO and adhesion molecules by the hepatic endothelium. The induction of iNOS and the inducible cytotoxic effect of LPS appear to be primarily located within the TPV region of the liver acinus.

Keywords: Tumour cell cytotoxicity; Apoptosis; Microvascular adhesion molecules; Nitric oxide; Metastasis; Liver; Hepatic sinusoid, lipopolysaccharide; Endothelium

1. Introduction

Blood vessels constitute transit routes that facilitate the widespread dissemination of metastatic cancer cells. Organs with extensive capillary networks, such as bone, lung or liver, are common metastatic targets, arguably on the basis that they constitute sites where mechanical restriction of cancer cells in small-bore vessels can cause tumour cell arrest [1,2].

There is evidence that the functional properties of microvascular lining cells can also govern the metastatic process [3]. In forming hepatic metastases, circulating cells that enter the hepatic microvasculature, generally pass through the periportal zone and arrest in the hepatic sinusoids by mechanical restriction [4,5]. We have previously shown that this event triggers the release of a burst of nitric oxide (NO) by the liver, which, in turn, initiates cytotoxic processes of apoptosis and necrosis in 20–30% of the intravascular tumour cells. This leads to an inhibitory effect on the subsequent formation of tumour metastases [6]. However, in mice that have previously been treated with Interleukin-1α (IL-1α),

* Corresponding author. Tel.: +1-204-789-3338; fax: +1-204-789-3931.
E-mail address: worr@cc.umanitoba.ca (F.W. Orr).

0959-8049/02/$ - see front matter
PII: S0959-8049(02)00039-4

circulating cancer cells arrest in the terminal portal venule (TPV) region of the liver and these cells subsequently form more metastases in that region. These latter effects have been related to the expression of the endothelial adhesion molecules E-selectin, vascular cell adhesion molecule-1 (VCAM-1), and intercellular adhesion molecule-1 (ICAM-1) [4] which are inducible following intraperitoneal (i.p.) injection of lipopolysaccharide (LPS) [7].

The present study was designed to test the hypothesis that an exogenous microenvironmental modulator can enhance the cytotoxic properties of the liver. Lipopolysaccharide (1 mg/kg i.p.) upregulated the expression of hepatic microvascular iNOS [8], nitric oxide, and adhesion molecules [7,9]. The synergistic interaction of NO and adhesion molecules in the TPV region decreased tumour cell clearance, increased tumour cell apoptosis, and inhibited the formation of metastatic tumors by intrahepatic melanoma cells. These experiments demonstrate that regulating hepatic microvascular functions can control the cytotoxic or metastatic outcomes of intravascular melanoma cells in the liver.

2. Materials and methods

2.1. Materials

Female C57BL/6 mice, weighing 20–22 g, were purchased from Charles River (Montreal, QC, Canada) and housed according to the University of Manitoba guidelines. The murine B16F1 melanoma cell line (syngeneic to C57BL/6 mice) was obtained from the American Type Culture Collection (Rockville, MD, USA). LPS was obtained from Sigma (Oakville, ON, Canada, L-2637, lot 123H4024). Fluoresbrite carboxylate YG 0.05-μm microspheres (microsphere stock: 2.5% solids—latex) were purchased from Polysciences, Inc. (Warrington, PA, USA). Tissue culture media, antibiotics and trypsin-ethylenediamine tetra acetic acid (EDTA) were all purchased from Gibco BRL (Life Tehcnologies, Burlington, ON, Canada). Hamster anti-mouse ICAM-1, rat anti-mouse VCAM-1, fluorescein isothiocyanate (FITC) anti-mouse CD11a, phycoerythrin (PE) anti-mouse CD49d and isotype control antibodies (FITC rat IgG_{2a} and PE rat IgG_{2b}) were purchased from PharMingen Canada (Mississauga, ON, Canada). Cy™ 3-conjugated goat anti-hamster IgG and goat anti-rat IgG secondary antibodies, and normal goat serum were purchased from Jackson ImmunoResearch Laboratories, Inc. (West Grove, PA, USA) . Affinity purified polyclonal rabbit anti-mouse iNOS primary antibody was purchased from Transduction Laboratories (Lexington, KY, USA). Alkaline phosphatase-conjugated goat anti-rabbit IgG was from ICN Pharmaceuticals Inc. (Aurora, OH, USA). Purified rat anti-mouse CD11a (LFA-1 [αLβ2] α chain) and rat anti-mouse CD49d (integrin α_4) monoclonal antibodies were purchased from BD Biosciences (PharMingen).

2.2. Culture and fluorescent labelling of B16F1 melanoma cells

Eighty per cent confluent B16F1 cells cultured in α-Modified Eagle Medium (MEM) with 10% fetal bovine serum and 1% penicillin/streptomycin in a T75 culture flask (Corning) at 37 °C and 5% CO_2 were incubated with fluoresbrite carboxylate microspheres in Opti-MEM serum-reduced medium (150 μl microspheres/7.5 ml Opti-MEM) for 2.5 h. At the end of the labelling, the supernatant was removed. The cells were rinsed three times with Opti-MEM to wash off the unincorporated beads and left in α-MEM culture medium overnight to reduce cell aggregation upon detaching. The labelled cells were detached with trypsin-EDTA-phosphate-buffered solution (PBS) (1/2 dilution) at 37 °C for 5 min with frequent rocking of the flask. The cell suspension was transferred into a centrifuge tube and centrifuged at 170*g* at room temperature for 3 min in a bench-top centrifuge. The cell pellet was resuspended in saline and kept on ice before injection. The concentration of all cell suspensions was determined using trypan blue and a haemocytometer. The cell viability before and after the injection period, measured by trypan blue was 95.3±3.5% standard deviation (S.D.) in the study. The method has been previously detailed in Ref. [6].

2.3. Intramesenteric injection of melanoma cells and LPS administration

Surgery was performed under aseptic conditions between 11:00 and 18:00 hours. The mice were anaesthetised with avertin (2,2,2-tribromoethanol, Caledon Laboratories Ltd., Georgetown, ON, Canada, 30 mg/ml, 0.3 ml/mouse). The abdomen was cleaned with 70% ethanol and opened through a small midline incision (~10 mm). The intestine was gently retracted and one branch of the superior mesenteric vein was isolated by separating the connective tissue around the vein using forceps. Fluorescently labelled B16F1 cells (5×10^5/150 μl saline) were injected into the mesenteric vein (5–10 min), using a 30 G1/2 needle and 1-ml syringe. A small piece of Gelfoam Sterile Sponge (12–7 mm, Upjohn) was used to stop the bleeding at the end of the injection. LPS (1 mg/kg) was given directly i.p. at the end of cell injection (B16F1 + LPS group), or given i.p. without cell injection (LPS only group). The incision was sutured using synthetic absorbable sutures (3–0 Vicryl, Ethicon, Johnson & Johnson, Peterborough, ON, Canada). The mouse was allowed to recover with a plastic catheter inserted in the mouth to facilitate breathing. The liver was collected under anaesthesia between 0 and 24 h

after injection without perfusion, following which the animals were killed by anaesthetic overdose. The Bannatyne Campus Protocol Management and Review Committee at the University of Manitoba certified all of the animal protocols.

2.4. Detection of iNOS expression in the liver

Random frozen sections (15 μm) from LPS stimulated or B16F1 cell injected livers (0–48 h) were transferred into 24-well plates (Corning, 1 section/well), washed 2× with 0.01 M PBS, 20–30 min/wash, and treated with proteinase K (1 μg/ml proteinase K buffer, 7.44 g EDTA, 2.45 g Tris acid, 2.96 g Tris base in 400 ml ddH_2O, pH 8.3) for 30 min at room temperature to facilitate iNOS antigen exposure. The floating sections were then washed 3× in 0.01 M PBS, 10 min/wash, followed by overnight incubation with 300 μl primary antibody, rabbit polyclonal anti-mouse iNOS, 1/500 dilution in blocking solution (1% normal goat serum (NGS)/1% Triton X–100/2% bovine serum albumin (BSA)), with slow rocking, at room temperature in a humidified chamber. The sections were washed 3× with 0.01 M PBS, 20 min/wash, at room temperature with vigorous shaking. This was followed by incubation with the secondary antibody, alkaline phosphatase-conjugated goat anti-rabbit IgG, 1/1000 dilution in blocking solution (1% NGS/1% Triton X, 300 μl/well), for 2 h at room temperature with slow rocking. The sections were then washed 3× in 0.01 M PBS, 20 min/wash, with vigorous shaking. Detection of the secondary antibody was through substrate colour reaction with alkaline phosphatase [10]. The colour development was 8 min/slide and stopped in 0.01 M EDTA/0.01 M PBS. The sections were transferred onto the slides precoated with gelatin (Type A, Fisher Scientific, Nepean, ON, Canada) and chromium potassium sulphate (Sigma, Oakville, ON, Canada), and mounted with aqueous mounting medium Gel/Mount™ (biomeda corp., Foster City, CA, USA). The slides were analysed under the light microscope. Ten fields (100× magnification) per liver sample were analysed. The data were expressed as the mean (±S.E.) positive cells per field of all the samples per time-point.

2.5. Detection of NO production in the liver by electron paramagnetic resonance (EPR) spectroscopy

The methodology has been previously described in Ref. [6]. Briefly, the NO trapping agents diethyldithiocarbamate (DETC, 400 mg kg^{-1} in saline, i.p.) and $FeSO_4$/sodium citrate (40 mg kg^{-1}/200 mg kg^{-1} mixed in water, subcutaneous (s.c.)) were given to each mouse 30 min before obtaining the liver sample. The mouse was anaesthetised with avertin before sacrifice. Constant portions of the left lateral, medial left and right, and right lateral lobes of the liver were quickly removed (between 30 s and 1 min) onto a Petri dish, precooled on ice. The mouse was sacrificed by opening the diaphragm and heart or anaesthetic overdose. The liver was quickly sliced into smaller pieces, placed into a precooled 1 ml syringe, and transferred into a suprasil synthetic quartz tube with open ends (2.4 mm inner diameter, Heraeus Amersil, GA, USA) by pushing the tissue through an 18 G needle from the syringe. The quartz tube was then immediately placed into the liquid nitrogen until NO measurement by EPR spectroscopy. The remaining liver tissue was removed from the mouse and fixed in 1% paraformaldehyde for 24–48 h at 4 °C and frozen at −80 °C in Tissue Tek O. C. T. for later analysis of cell distribution and apoptosis.

EPR measurement of the trapped NO–Fe^{2+}–$(DETC)_2$ complex was performed at 115 K (−158 °C, Bruker Instruments, temperature controller Model ER-4111, Germany). The spectra were measured with a Varian Associates Model E-12 EPR spectrometer, operating at 9.025 GHz with 100 kHz modulation that was interfaced with a Nicolet Instruments Model 1180 computer and Model 2090 digital oscilloscope. The instrument settings were: microwave power 5 mW, modulation amplitude 5 G and a scan range of 500 or 1000 Gauss (G). The concentration of the NO–Fe^{2+}–$(DETC)_2$ complex in each sample was proportional to the signal amplitude (peak-to-peak) of the triplet-hyperfine structure (hyperfine splitting of 13 G) observed at $g = 2.04$.

2.6. Melanoma cell distribution and clearance from the liver

As described before in Ref. [6], 15 μm frozen sections from constant regions in three different lobes at three different planes of the left lateral, medial and right lateral lobes per liver were cut, transferred onto slides and mounted with Gel/Mount™. Ten microscopic fields per lobe (100× magnification) with the highest cell numbers were counted to determine the number of fluorescently-labelled B16F1 cells in both the terminal portal venule and sinusoidal regions. To increase the sampling area, the data were expressed as the sum of the three mean values of absolute cell numbers from each lobe. Each mean was the average of the 10 counts from the 10 fields in each lobe.

2.7. Double labelling of adhesion molecules and fluorescent melanoma cells in the liver

For detection of adhesion molecules on the hepatic microvasculature or on melanoma cells after cell injection, the resected livers were fixed in 1% paraformaldehyde (BDH Laboratory Supplies, Poole, UK) for 24–48 h and frozen at −80 °C in Tissue Tek O. C. T. (Sakura Finetek USA, Inc., Torrance, CA, USA) without cryo-protection in 30% sucrose in order to preserve the fluorescent-labelling of the melanoma cells and achieve optimal double label of adhesion molecule expression and tumour cells

in vivo. As previously described, a floating-section method was used to stain sections of the liver tissue (40 μm thickness) [7]. Confocal scanning laser microscopy (Molecular Dynamics) was used to analyse the data.

2.8. Flow cytometry

The expression of counter receptors of adhesion molecules (VCAM-1/VLA-4 and ICAM-1/LFA-1) on melanoma cells was detected using flow cytometry. Eighty per cent confluent B16F1 cells in culture were treated with 10 and 20 μg/ml LPS for 8 h. The cells were detached with trypsin-EDTA and pelleted by centrifugation in a bench-top centrifuge. The cell pellet was washed once with 0.01 M PBS–2% fetal bovine serum (FBS) and spun down. The pellet was resuspended in PBS–2% FBS and counted with trypan blue; cells for these experiments demonstrated 100% viability. Final cell suspension was made at 5×10^6/ml PBS–2% FBS. 100-μl cell suspension (5×10^5 cells) was removed into each tube for various antibody labellings. Five μg of counter receptor antibodies and their isotype controls was added into individual tubes, mixed and left on ice in the dark for 40 min with occasional shaking of the tubes. At the end of the labelling, 3 ml cold PBS-FBS per tube was added. The cells were spun down. The supernatant was aspirated. One ml/tube of 1% paraformaldehyde was added, mixed and kept on ice in the dark for the following flow cytometry analysis.

Flow cytometry analysis was performed on a Beckman Coulter EPICS ALTRA cell sorter with laser excitation set at 488 nm. The EXPO2 software provided with the system was employed for data acquisition and initial data analysis. Forward versus side scatter histograms were used to gate on single intact cells. The data was collected in listmode format with the subsequent analysis based on 10 000 cells satisfying the light scatter criteria. The fluorescence signals from each cell were split with a 550 nm dichroic long pass filter, with the PE and FITC-derived fluorescence detected through 575 and 525 nm bandpass filters, respectively. Immunoglobulin conjugates matched for isotype and fluorochrome were used as controls to assess autofluorescence and non-specific staining.

2.9. Detection of in vivo apoptosis of B16F1 melanoma cells by in situ DNA end-labelling

The optimised methodology has been described in Ref. [6]. Briefly, frozen sections (17 μm) were obtained from random sampling areas in the livers of each treatment group. *In situ* DNA end labelling (TUNEL assay) was performed on the sections that contained injected fluorescent microsphere-labelled melanoma cells, using a digoxigenin-peroxidase detection system (ApopTag S7100 Kit, Intergen Company, Purchase, NY, USA). To achieve optimal double-labelling with cytoplasmic fluorescent microspheres and nuclear apoptotic staining in the melanoma cells, proteinase K digestion (20 μg/ml), 15 min at room temperature followed by two washes with dd H_2O, was performed before permeabilising the cells with ethanol/acetic acid (2:1 v/v, Manufacturer's instructions). Terminal deoxynucleotidyl transferase incubation was performed overnight in a humidified chamber at 37 °C, with a subsequent 1 h anti-digoxigenin peroxidase conjugate incubation at room temperature in a humidified chamber. Peroxidase substrate colour was developed for 12 min per slide without any other 'Counter Stain Specimen' and 'Mount Specimen' steps thereafter (Manufacturer's instruction) to prevent the quenching of fluorescence of the microspheres by organic solvents. The slides were mounted with Gel/Mount™.

The number of both single-fluorescent and doubly labelled cells (fluorescent-ApopTag DNA end-labelling) and their locations in the TPV or sinusoid were scored in each sample using a microscope with dual fluorescent and incandescent illumination. To achieve a constant sampling area, we quantified all tumour cells located in 5 fields/section, 10 sections per sample, under a 100× magnification. The percentage of apoptotic melanoma cells in the TPV or sinusoidal region was calculated as: Apoptotic tumour cells/region (%) = 100×(Doubly-labelled cells)/Total cells (Doubly-labelled + Single fluorescently-labelled) in the region.

2.10. Liver metastasis

Two groups of mice received intramesenteric injections of B16F1 cells only (5×10^5/150 μl saline, non-labelled) or B16F1 cells + LPS (1 mg/kg, i.p., at the end of injection) and were allowed to survive for 14 days with postsurgical care according to the standards of the University of Manitoba. The mice were then sacrificed by anaesthetic overdose and their livers were removed. Liver metastasis was quantified both macroscopically and microscopically [6].

2.11. Statistical analysis

All samples were scored blindly. Data were analysed by one-way ANOVA followed by Tukey's Honestly Significant Difference (HSD) test for pairwise comparisons, or by three-way ANOVA with repeated measures followed by Planned Comparison to compare specific groups of interest.

3. Results

3.1. iNOS and NO expression

Strong induction of NO was detected 8 h after i.p. injection of LPS and following injection of both B16F1

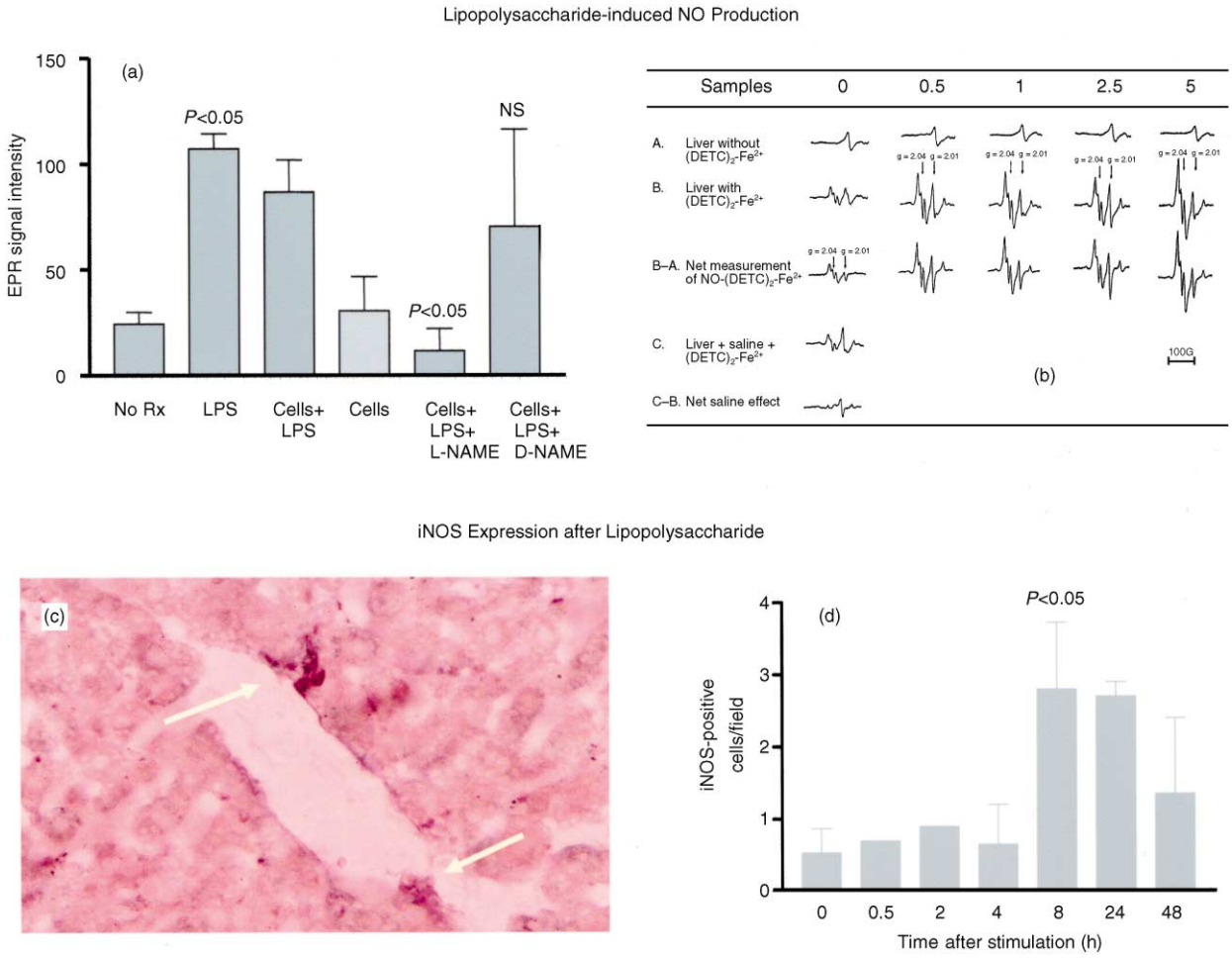

Fig. 1. Induction of hepatic NO and iNOS by LPS. Panel (a) NO production 8 h after injection of 1 mg/kg LPS and B16F1 melanoma cells ($n = 3$–5 mice per group). Panel (b) EPR spectra showing dose-dependent production of hepatic NO after LPS (0–5 mg/kg). (EPR amplitude at 0 mg/kg = 33 units; amplitude at 5 mg/kg = 135 units). Panel (c) Immunohistochemical detection of iNOS-positive microvascular cells in the terminal portal venular region (×400). Panel (d) Quantitative immunohistochemical analysis of iNOS expression (mean ± S.E.M.). Rx, therapy; NS, non-significant.

cells and LPS (Fig. 1a). We confirmed our previous observation that there is a transient burst of hepatic NO within 5 min after the injection of melanoma cells into the portal venous circulation [6] (data not shown), but NO expression was not increased above basal levels when measured 8 h later. Treatment of mice with the non-selective NO synthase inhibitor L-NAME blocked the induction of NO that followed the injection of LPS and cells, while its inactive enantiomer D-NAME had no significant effect. The level of NO production after LPS was dose-dependent (Fig. 1b). Following the injection of LPS, iNOS expression was increased in the periportal sinusoidal lining cells (Fig. 1c) and could be detected up to 48 h thereafter (Fig. 1d). iNOS induction was not seen in the mice injected with cells alone.

3.2. *Effects of LPS treatment on the distribution and clearance of arrested intrahepatic melanoma cells*

From 0 to 4 h after the B16F1 cell injection, there was a decrease in the number of cells per unit area in mice injected with tumour cells alone and in mice injected with tumour cells and LPS. In both groups, approximately 2/3 of the melanoma cells were located in the sinusoids at these time-points. Approximately 1/3 of the cells were found in the terminal portal venules. However, between 4 and 8 h, there was a significant increase in the number of cells per unit area in animals injected with LPS, while the number of cells per unit area continued to decrease in animals injected with tumour cells only. The increase in cell number after LPS was seen in both the terminal portal venules and sinusoidal regions (Fig. 2).

The increase in B16F1 cells after LPS seemed to suggest that intravascular melanoma cells may continue to circulate and arrest in the liver. To seek evidence for this, we examined the arterial blood harvested from the left ventricle of LPS-treated mice 6–8 h after intramesenteric injection of the B16F1 cells as a potential source of these cells. By fluorescence microscopy a median of 90 (range = 20–725) fluorescently labelled melanoma cells were identified in 1 ml of peripheral

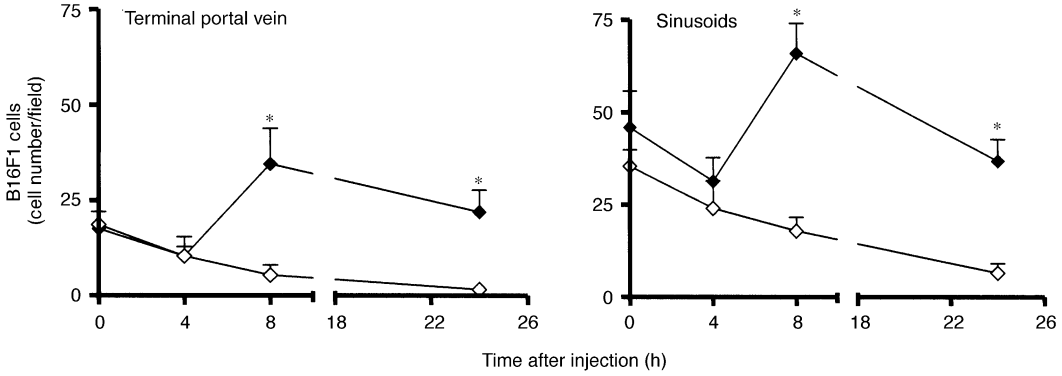

Fig. 2. Effects of LPS on the distribution and clearance of B16F1 melanoma cells in the terminal portal vein region and sinusoids. Data represent means±S.E.M. $n=3$ mice/time-point. *$P<0.01$–0.05 (three-way ANOVA, repeated measures followed by planned comparisons). ◇-◇: B16 melanoma cells only ◆-◆: B16 melanoma cells + LPS.

arterial blood harvested from each of three mice. Accumulation of cells in the terminal portal venules of LPS-treated mice corroborated the observations we have made previously by intravital microscopy in animals treated with the cytokine interleukin-1α prior to injection of the cells into the portal venous circulation [4].

3.3. Effects of cell arrest and LPS on hepatic microvascular adhesion molecule expression

To further investigate the reasons for the effect of LPS on cell retention and clearance, we used single and dual-label fluorescent immunohistochemistry to examine the expression of adhesion molecules ICAM-1 and VCAM-1 by the hepatic microvasculature. In control mice, basal ICAM-1 was detected in the periportal regions of the hepatic lobules and also in the midzone regions although here expression was at a lower level. In these animals, VCAM-1 expression was restricted to the periportal regions (Table 1). Increased expression of both ICAM-1 and VCAM-1 was seen in the periportal and midzone regions 8 h after injecting 5×10^5 B16 melanoma cells only into the portal circulation. The induction was primarily observed at the sites of tumour cell arrest. VCAM-1 expression was essentially limited to the site of tumour cell arrest, while ICAM-1 expression was more generalised and greater in magnitude (Fig. 3a and b). There were positive correlations between the number of melanoma cells that had arrested per unit area and the levels of expression of both adhesion molecules (Table 1). Both ICAM-1 and VCAM-1 were expressed to a greater degree after the animals were injected with LPS (1 mg/kg i.p.). Expression of both adhesion molecules was enhanced following combined injection of cells and LPS, compared with cell injection only, although the levels of expression were slightly less than those following LPS alone (Fig. 3c and d; Table 1).

We also examined the expression of LFA-1 and the α4 integrin on the B16F1 cells to determine whether the altered patterns of cell arrest could be related to an effect of LPS on the expression of these counterreceptors for vascular ICAM-1 and VCAM-1. Flow cytometry demonstrated basal VLA-4 expression in 98% of the cultured melanoma cells, while approximately 1.5% of the cells expressed LFA-1. These expression levels were changed by $<2\%$ following 8 h culture of the cells with 10–20 μg/ml LPS. Using fluorescent immunohistochemistry to examine the expression of these counterreceptors on melanoma cells within the hepatic microvasculature, we detected LFA-1 expression on $16\pm2\%$ of the cells retained in the liver 8 h after cell injection only; $11\pm3\%$ expressed the α4 integrin. In cells and LPS-injected mice, these values were 8 ± 2 and $8\pm4\%$, respectively. Thus, using these two detection methods, neither LFA-1 expression nor α4 integrin expression on the melanoma cells was demonstrably upregulated by treatment with LPS *in vitro* or *in vivo*.

3.4. Effects of LPS on B16F1 melanoma cytotoxicity

We quantified B16F1 apoptosis in vivo by DNA end labelling in order to examine the potential cytotoxic consequences of the LPS-induced melanoma cell retention and enhanced local iNOS (NO) expression in the TPV region. Whereas our previous observations showed a cytotoxic effect on melanoma cells in the sinusoids, dependent upon an NO burst occurring immediately after cell arrest [6], the present experiments demonstrated an enhanced cytotoxic effect on the melanoma cells located in the terminal portal venules (Fig. 4). In mice injected with cells alone, the rates of apoptosis were higher in the sinusoids than in the terminal portal venules. In contrast, in mice that had been given LPS, the percentage of apoptotic cells in the terminal portal venules was significantly higher than in the controls although the rates of apoptosis in the sinusoids were not significantly affected by LPS treatment in the same time-points. Following LPS, the proportion of apoptotic

Table 1
Effects of cell arrest and LPS on the expression of ICAM-1 and VCAM-1 by the hepatic microvasculature

Treatment	ICAM-1		VCAM-1	
	Units of expression per high power field[a]			
	Periportal	Midzone	Periportal	Midzone
No treatment group	8±1	3±1	4±2	0
Cell injection only[b]	25±6	30±6	10±5	7±3
LPS only	65±6	61±7	21±7	8±2
LPS and cells	39±3	47±6	18±4	12±5

[a] Immunohistochemical quantification performed on samples harvested 8 h after treatment.
[b] 5×10^5 B16F1 melanoma cells in 150 μl saline were injected into a mesenteric vein of C57 Bl/6 mice. Immunohistochemical analysis of adhesion molecule expression was done on samples of liver harvested 8 h afer cell injection. Correlations between the number of arrested cells per unit area and expression of adhesion molecules were:

ICAM-1, periportal zone	r = 0.48	$P = 0.028$
ICAM-1, midzone	r = 0.68	$P = 0.001$
VCAM-1, periportal zone	r = 0.43	$P = 0.065$
VCAM-1, midzone	r = 0.45	$P = 0.040$

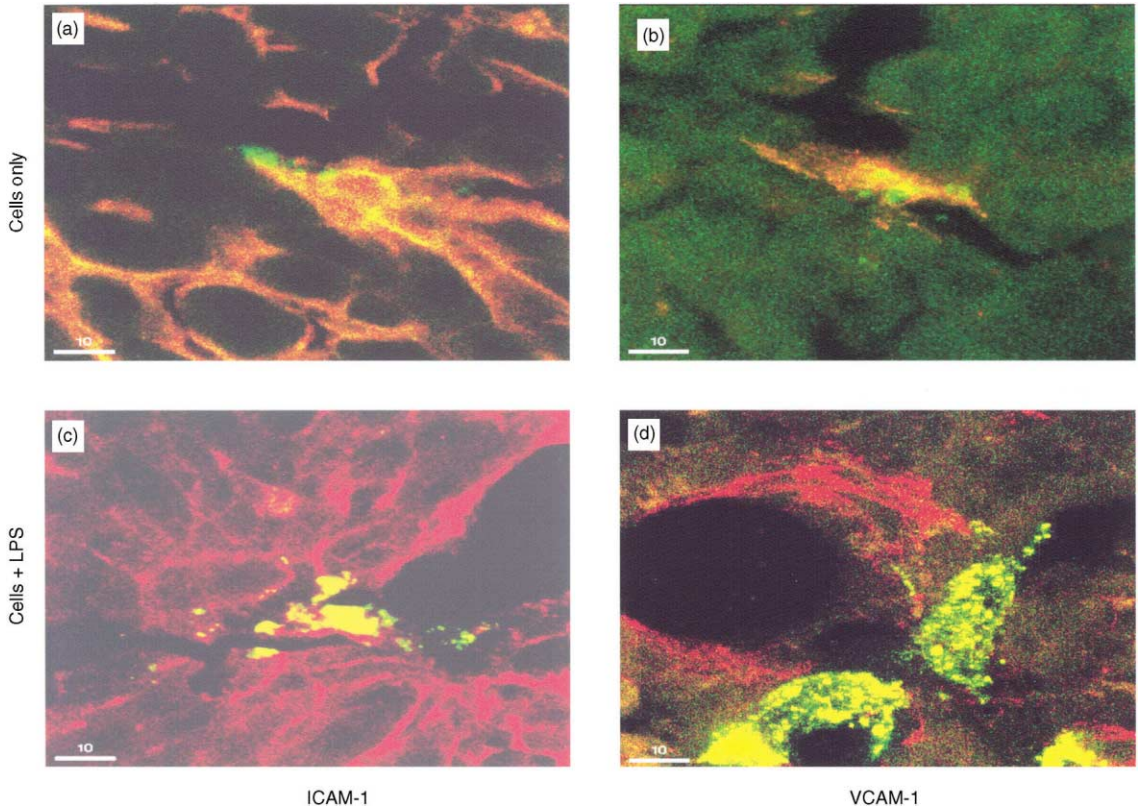

Fig. 3. Expression of ICAM-1 and VCAM-1, 8 h after injection of B16F1 cells only or B16F1 cells and LPS. Five$\times10^5$ microsphere-labelled B16F1 cells were injected into the portal venous circulation alone or followed by an i.p. injection of 1 mg/kg LPS. In mice injected with cells only, dual-labelled confocal scanning laser microscopic images show ICAM-1 (panel a) and VCAM-1 (panel b) induction (Cy3, red) at the site of arresting fluorescent (green) B16F1 cells in the sinusoids. Enhanced induction of ICAM-1 and VCAM-1 in mice injected with B16F1 cells and LPS are shown in panels c and d, respectively.

melanoma cells in the terminal portal venules reached similar levels to those in the sinusoids of the control animals. There was a positive correlation between the level of NO and rate of tumour cell apoptosis at 8 h (r = 0.58, $P = 0.10$).

3.5. *Effects of LPS on metastasis*

The livers of the mice were examined 14 days after tumour cell injection to determine if the LPS treatment had an effect on the formation of metastases by the

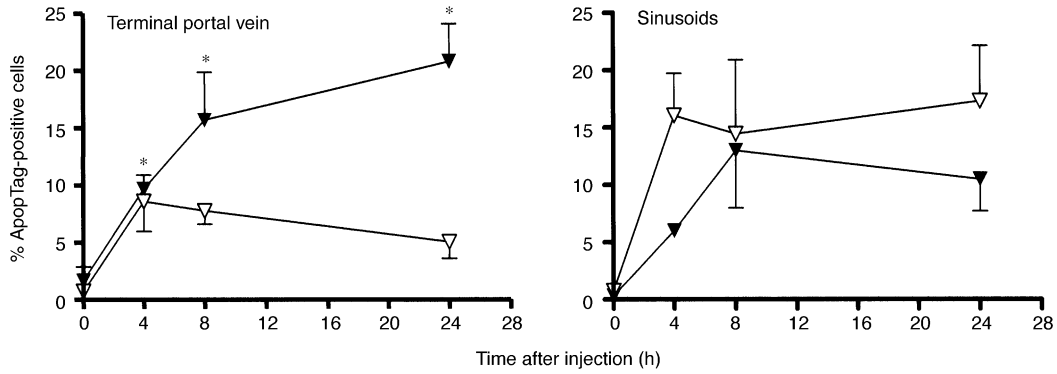

Fig. 4. Effects of LPS treatment on melanoma cell cytotoxicity. The percentage of apoptotic B16F1 cells was calculated by DNA end-labelling (means ± S.E.M.). $n = 3$–4 mice/time-point $^*P < 0.05$ (three-way ANOVA, repeated measures followed by planned comparisons). ▽-▽: B16 melanoma cells only ▼-▼: B16 melanoma cells + LPS.

Table 2
Liver surface metastasis formed at day 14 following intramesenteric injection of B16F1 cells

Observation	Treatment group		
	B16 cells only	B16 cells + LPS	
Number of mice	8	5	
Lobes with confluent tumour[a]	2 (0–3)	0 (0–1)	$P = 0.046$
Liver weight (g)	2.5 (1.3–4.6)	1.8 (1.4–2.3)	$P = 0.064$
% Histological fields with tumour	56 ± 5	27 ± 12	$P = 0.022$

[a] Left lateral, medial and right lateral lobes were evaluated macroscopically in each mouse 14 days after the melanoma cell injection. Data are expressed as medians and ranges. The Mann–Whitney test was used for the statistical analysis.

melanoma cells. Table 2 demonstrates that the control animals had a significantly greater tumour burden than the LPS group as measured by the number of lobes replaced by confluent metastatic tumour ($P = 0.046$), liver weight ($P = 0.064$), and histological areas occupied by tumour ($P = 0.0215$).

4. Discussion

These experiments were conducted to challenge our previous observations that the hepatic microvasculature can regulate the metastasis of cancer cells to the liver. Our data demonstrate that bacterial endotoxin is a potent microenvironmental stimulus that can simultaneously upregulate the expression of hepatic endothelial adhesion molecules and increase hepatic NO production. This study corroborates previous evidence that hepatic microvascular adhesion molecules can cause circulating B16 melanoma cells to arrest in zone 1 of the hepatic acinus [4] and that liver-derived NO can induce apoptosis or necrosis in these cells [6]. Here, we show for the first time that, in concert, these two events have a net inhibitory effect on the ability of intravascular B16 melanoma cells to form metastases within the liver.

In previous work, we had shown that the arrest of circulating intravascular tumour cells in the sinusoids causes the release of liver-derived NO within 5 min of cell injection, as a result of mechanical arrest and independent of iNOS induction [6]. In contrast to this, the production of NO 8 h after administration of LPS was dose-dependent and correlated with the induction of iNOS in the terminal portal venules and periportal sinusoids (acinar zone 1). Neither iNOS nor NO were increased 8 h after injecting cells alone. These observations document the existence of iNOS-dependent and iNOS-independent mechanisms for the production of NO by the liver microvasculature. We postulate that the iNOS-independent mechanisms are likely related to constitutive NOS (eNOS) and are probably responsible for the early burst of NO resulting from mechanical transduction due to the arrest of tumour cells. Additional studies are underway to examine this.

Since we observed altered patterns of cell retention and clearance in the LPS-treated mice, we also examined the effects of LPS treatment on the expression of adhesion molecules by the microvasculature and the tumour cells. Arrest of the B16 melanoma cells within the hepatic microcirculation was associated with the induction of both VCAM-1 and ICAM-1 at the site of tumour arrest. VCAM-1 induction was limited to the microvasculature adjacent to the melanoma cells, while the magnitude of ICAM-1 induction was greater, extending to adjacent sinusoidal lining cells. There was a positive correlation between the number of arrested cells and the degree of expression of both adhesion

molecules. These results extend the observation that upon entry into the hepatic circulation, tumour cells can initiate expression of a molecular cascade leading to the induction of E-selectin expression on the sinusoidal endothelium [11] and support the hypothesis that induction of adhesion molecules may contribute to the liver-colonising potential of tumour cells, perhaps by promoting the firm attachment of these cells to the microvascular surface.

LPS administration stimulated the expression of hepatic microvascular VCAM-1 and ICAM-1, but not the vascular cell counterreceptors for the α4β1integrin and αLβ2 [12,13]. Expression of ICAM-1 and VCAM-1 was associated with accumulation of intravascular metastatic cells within the liver. While B16F1 cells were cleared from both control and LPS-treated mice during the first 4 h after injection, by 8 h, the number of tumour cells began to increase in the LPS-treated mice, especially within the terminal portal venules. Thereafter, tumour cells continued to be cleared in control mice and to increase in mice treated with LPS. The timing of the LPS-related increase in tumour cell adhesion is consonant with the kinetics of adhesion molecule expression after LPS [7] and with the evidence that both ICAM-1 and VCAM-1 mediate attachment of B16 melanoma cells to the microvasculature in zone 1 of the liver acinus [4]. Since the total number of tumour cells counted in the liver at 8 h in LPS-treated mice was greater than the number counted immediately after injection, we questioned whether the increase might be due to the arrival of additional melanoma cells into the microvascular bed during this interval. In order to identify a potential source of such cells, we examined the arterial blood of the tumour-bearing mice and determined that morphologically intact melanoma cells could be found there. Our results indicate that if vascular adhesion molecules have been induced, circulating melanoma cells are preferentially trapped within the terminal portal venules and then have a reduced rate of subsequent clearance from the liver. The altered clearance of cells after LPS did not appear to be due to an effect of LPS on the tumour cell adhesion molecules since neither the expression of α4β1 nor αLβ2 by the melanoma cells was altered significantly after exposure of the cells to LPS *in vitro* or in LPS-treated mice. It is interesting that we found a greater proportion of αLβ2-expressing cells *in vivo* than *in vitro*. This could reflect a role for αLβ2 in attachment of the melanoma cells to the hepatic microvasculature and the selection of this cell population in the metastatic process. Differences between the levels of expression *in vitro* and *in vivo* might also be due to the differing sensitivities of flow cytometry and immunohistochemistry.

The localised induction of iNOS in the acinar zone 1 correlated also with enhanced apoptosis of cells in this anatomical region. Enhanced cytotoxicity after LPS was not seen in the sinusoids where we did not see as great an induction of iNOS. The positive correlation between NO levels and apoptosis also implicates NO as a mediator of apoptosis.

It has been established that activated sinusoidal lining cells can induce mitochondrial dysfunction and membrane damage in tumour cells through the release of NO both *in vitro* and *in vivo* [14,15]. The effects of NO on the progression and metastatic behaviour of tumour cells are variable [16]. In some cells, metastasis is inhibited by the cytotoxic effects of host-derived NO [17,18]. In other cells, endogenous or host-derived NO can promote the expression of metastatic phenotypes such as migration, invasiveness, or the ability of the cells to stimulate angiogenesis [19,20]. The B16F1 cells used in our studies are NO-sensitive and undergo apoptosis and/or necrosis following a brief exposure to NO. Using EPR spectroscopy, we have not detected NO production by these cells [6]. The antimetastatic effects of NO may not be completely dependent on a cytotoxic effect. We do not think it likely that the increased adherence of B16F1 cells to the terminal portal venules results from LPS-driven NO production since NO has been reported to reduce the attachment of tumour cells to the endothelium [21]. Further experiments using NO inhibitors and NOS knockout mice are being done to resolve this. The applicability of these mechanisms to other tumour cell types has not been determined.

Although LPS induced both adhesion molecule expression and NO release, the net effect of these two events was an increased killing of B16F1 cells in the terminal portal venules and periportal sinusoids and a decrease in the subsequent metastatic burden by these cells. The apparent paradox between increased adhesion of cells to the endothelium and increased apoptosis suggests the possibility that attachment of tumour cells to the endothelial NO donor may facilitate the cytotoxic action of NO. Our data suggest that by trapping more cells and inducing NO release in the periportal zone of the liver lobule, LPS had a net cytotoxic and antimetastatic effect. The results are consistent with the principle that the functional properties of the hepatic microvasculature are heterogeneous, synergistic, zonal in distribution, and differentially regulated [22]. Thus, the cytotoxic properties of the midzone and central sinusoids were not enhanced by LPS, but rather, LPS slightly decreased the percentage of apoptotic cells distributed in the sinusoids possibly relating to their increased clearance [23].

In summary, these observations reaffirm the existence of mechanisms by which hepatic microvascular functions can regulate the metastatic outcome of intravascular cancer cells within the liver and they show that these mechanisms are susceptible to modulation by environmental factors.

Acknowledgements

This work was supported by grants from the Medical Research Council of Canada and the Canadian Institutes for Health Research (MT (MOP)-14356 and MT-14477).

References

1. Batson OV. The role of vertebral veins in metastatic processess. *Ann Intern Med* 1942, **16**, 38–46.
2. Weiss L. The biomechanics of cancer cell traffic, arrest, and intravascular destruction. In Orr FW, Buchanan MR, Weiss L, eds. *Microcirculation in Cancer Metastasis*. CRC Press, Boca Raton, 1991, 131–144.
3. Orr FW, Wang HH. Tumor cell interactions with the microvasculature: a rate-limiting step in metastasis. *Surg Oncol Clin N Am* 2001, **10**, 357–381.
4. Scherbarth S, Orr FW. Intravital videomicroscopic evidence for regulation of metastasis by the hepatic microvasculature: effects of interleukin-1alpha on metastasis and the location of B16F1 melanoma cell arrest. *Cancer Res* 1997, **57**, 4105–4110.
5. Groom AC, MacDonald IC, Schmidt EE, Morris VL, Chambers AF. Tumour metastasis to the liver, and the roles of proteinases and adhesion molecules: new concepts from in vivo videomicroscopy. *Can J Gastroenterol* 1999, **13**, 733–743.
6. Wang HH, McIntosh AR, Hasinoff BB, *et al*. B16 melanoma cell arrest in the mouse liver induces nitric oxide release and sinusoidal cytotoxicity: a natural hepatic defense against metastasis. *Cancer Res* 2000, **60**, 5862–5869.
7. Wang HH, Nance DM, Orr FW. Murine hepatic microvascular adhesion molecule expression is inducible and has a zonal distribution. *Clin Exp Metastasis* 1999, **17**, 149–155.
8. Aono K, Isobe K, Kiuchi K, *et al*. In vitro and in vivo expression of inducible nitric oxide synthase during experimental endotoxemia: involvement of other cytokines. *J Cell Biochem* 1997, **65**, 349–358.
9. Vidal-Vanaclocha F, Alvarez A, Asumendi A, Urcelay B, Tonino P, Dinarello CA. Interleukin 1 (IL-1)-dependent melanoma hepatic metastasis in vivo; increased endothelial adherence by IL-1-induced mannose receptors and growth factor production in vitro. *J Natl Cancer Inst* 1996, **88**, 198–205.
10. Meltzer JC, Grimm PC, Greenberg AH, Nance DM. Enhanced immunohistochemical detection of autonomic nerve fibers, cytokines and inducible nitric oxide synthase by light and fluorescent microscopy in rat spleen. *J Histochem Cytochem* 1997, **45**, 1–12.
11. Khatib AM, Kontogiannea M, Fallavollita L, Jamison B, Meterissian S, Brodt P. Rapid induction of cytokine and E-selectin expression in the liver in response to metastatic tumor cells. *Cancer Res* 1999, **59**, 1356–1361.
12. Anasagasti MJ, Alvarez A, Martin JJ, Mendoza L, Vidal-Vanaclocha F. Sinusoidal endothelium release of hydrogen peroxide enhances very late antigen-4-mediated melanoma cell adherence and tumor cytotoxicity during interleukin-1 promotion of hepatic melanoma metastasis in mice. *Hepatology* 1997, **25**, 840–846.
13. Neelamegham S, Taylor AD, Burns AR, Smith CW, Simon SI. Hydrodynamic shear shows distinct roles for LFA-1 and Mac-1 in neutrophil adhesion to intercellular adhesion molecule-1. *Blood* 1998, **92**, 1626–1638.
14. Fukumura D, Yonei Y, Kurose I, *et al*. Role in nitric oxide in Kupffer cell-mediated hepatoma cell cytotoxicity in vitro and ex vivo. *Hepatology* 1996, **24**, 141–149.
15. Edmiston KH, Shoji Y, Mizoi T, Ford R, Nachman A, Jessup JM. Role of nitric oxide and superoxide anion in elimination of low metastatic human colorectal carcinomas by unstimulated hepatic sinusoidal endothelial cells. *Cancer Res* 1998, **58**, 1524–1531.
16. Chung HT, Pae HO, Choi BM, Billiar TR, Kim YM. Nitric oxide as a bioregulator of apoptosis. *Biochem Biophys Res Commun* 2001, **282**, 1075–1079.
17. Shi Q, Xiong Q, Wang B, Le X, Khan NA, Xie K. Influence of nitric oxide synthase II gene disruption on tumor growth and metastasis. *Cancer Res* 2000, **60**, 2579–2583.
18. Wang B, Xiong Q, Shi Q, Le X, Abbruzzese JL, Xie K. Intact nitric oxide synthase II gene is required for interferon-beta-mediated suppression of growth and metastasis of pancreatic adenocarcinoma. *Cancer Res* 2001, **61**, 71–75.
19. Jadeski LC, Hum KO, Chakraborty C, Lala PK. Nitric oxide promotes murine mammary tumour growth and metastasis by stimulating tumour cell migration, invasiveness and angiogenesis. *Int J Cancer* 2000, **86**, 30–39.
20. Wang B, Xiong Q, Shi Q, Tan D, Le X, Xie K. Genetic disruption of host nitric oxide synthase II gene impairs melanoma-induced angiogenesis and suppresses pleural effusion. *Int J Cancer* 2001, **91**, 607–611.
21. Kong L, Dunn GD, Keefer LK, Korthuis RJ. Nitric oxide reduces tumor cell adhesion to isolated rat postcapillary venules. *Clin Exp Metastasis* 1996, **14**, 335–343.
22. Wisse E, Braet F, Luo D, *et al*. Structure and function of sinusoidal lining cells in the liver. *Toxicol Pathol* 1996, **24**, 100–111.
23. Bayon LG, Izquierdo MA, Sirovich I, Van Rooijen N, Beelen RH, Meijer S. Role of Kupffer cells in arresting circulating tumor cells and controlling metastatic growth in the liver. *Hepatology* 1996, **23**, 1224–1231.